JOURNAL OF MATERIALS SCIENCE 29 (1994) 2931–2938

Steady and oscillatory flows of silicon-polypropylene ceramic compounds

A. I. ISAYEV, XIYUN FAN*
Institute of Polymer Engineering, The University of Akron, Akron, OH 44325-0301, USA

The rheological properties of a ceramic moulding compound, silicon powder with a polypropylene binder system, were studied using a Rheometrics mechanical spectrometer RMS-800 and an Instron capillary rheometer. The study included steady simple shear flow, transient start-up shear flow, stress relaxation upon cessation of steady shear flow, stress relaxation after a sudden shear displacement, and dynamic oscillatory shear flow. Yield behaviour was observed in both steady-shear and dynamic measurements. The empirical Cox–Merz rule which is usually applicable to polymer melts and solutions was found to be invalid for this material. The modified Cox–Merz rule, in which the apparent viscosity versus shear rate is equal to the complex viscosity versus the shear-rate amplitude in the highly non-linear region, was found to be valid for this material system. A series of anomalous phenomena were also observed during the shear-flow experiments including work hardening in the very-low-shear-rate region, stress oscillation in the high-shear-rate region, and stress relaxation followed by substantial stress growth in the stress-relaxation measurements.

1. Introduction

Ceramic-filled materials are typical examples of a disperse system. Their rheology is very complex. Ceramic injection-moulding compounds exhibit a yield stress [1–4] which must be overcome before the materials flow. The existence of a yield stress is due to the presence of a coagulated structure formed by the ceramic particles, and it is dependent on the particle shape and packing density [3]. Once the material begins to flow, its viscosity depends on temperature, shear rate [1, 4] and time [5, 6].

The flow behaviour of ceramic compounds can be successfully described by either the Bingham [7] or pseudoplastic-flow model [1, 6, 8] or by a variant of the Casson equation [4]. Edirisinghe and Evens [9] measured the rheological properties of nine ceramic injection-moulding compositions based on polypropylene with a fixed silicon-powder loading, and they found that all the formulations showed pseudo-plastic behaviour over the range of shear rates 100–1000 s^{-1}. However, it was quite possible for an apparently pseudo-plastic system to become dilatant at high shear rates. Litman *et al.* [10] noted that at a 50 vol % loading the mixture showed pseudo-plastic behaviour, while at 70 vol % it showed dilatant behaviour.

Umeya [11] stated that the rheological behaviour of a ceramic mixture for injection moulding was viscoelastic–plastic, which is similar to that of a slurry. The flow characteristics of such a system can be expressed by an extended Ostwald-flow model. In a wide shear rate range, there exists three Newtonian-flow regions. Before the first Newtonian region is the yield region. Between the first and second Newtonian regions is the pseudo-plastic-flow region and between the second and third Newtonian regions is the dilatant-flow region. All these behaviours are related to the change of the particle flocculation structure during flow.

Isayev [4] reported appreciable slip at the wall of a silicon compound by using a knurled-surface rotation member in addition to the usual smooth surface member in a co-axial cylinder viscometer. Oscillation of pressure or stick–slip behaviour during the capillary flow of pure or particle-filled polymer melts was reported by several researchers [12–15]. To the best of our knowledge such effects were not reported for ceramic compound systems.

An abnormal flow phenomenon was described by Vinogradov and Malkin [16] on a dispersed system exhibiting the flow curve with a yield value. When a typical plastic disperse system is subjected to a constant rate of deformation, a work-hardening effect might appear due to the strength of the existing particle skeleton. In the very-low-shear-rate region (usually, $\dot{\gamma} < 10^{-6}\ s^{-1}$) below a certain critical value, $\dot{\gamma}_a$, the dependencies $\dot{\gamma}(\tau)$ are monotonic. At the attainment of $\dot{\gamma}_a$ there is a characteristic value of the shear stress, τ_y, corresponding to the yield stress. The transition through the yield stress is accompanied by a catastrophic breakdown of the structural skeleton,

* *Present address:* Washington Research Center, W. R. Grace Company, Columbia, MD 21044, USA.

0022–2461

such that the shear stress even decreases, with increasing shear rate, to a minimum value. This phenomenon was called the *super-anomalous viscosity*. Then the shear stress rapidly increases as the shear rate further increases, and the system shows a typical non-Newtonian behaviour.

The evolution of composite structure with time was described by White [17]. In particular, two mechanisms were pointed out: a separation of the particle agglomerates from each other with subsequent dispersion, and the break up of individual agglomerates into particles during flow. The action of stresses in dispersing the particulate aggregates was discussed by several researchers [18–20]. Umeya [11] made a detailed explanation of the flow pattern in terms of the structure flocculation. The role of interparticular Van der Waals forces in concentrated suspension flows was given by Tsai and Zammouri [21].

Stress relaxation is a very complex process in particle-filled polymer melts. Some authors have argued that in such a material system the stress relaxes to a finite value, rather than to zero, after cessation of the steady-state flow [22–24]. Chan and Powell [24] studied the effect of the concentration of spherical glass beads on the stress-relaxation curves. They found that the shear stresses decreased monotonically from their steady-state values. An interesting stress-relaxation phenomenon was observed by Glushkov *et al.* [25]. They found that after steady shear flow at a low shear rate the stress-relaxation curves were different at different shear rates for a polybutadiene elastomer filled with calcium chloride and carbon black. The stress varied monotonically with time and finally tended to the constant residual stress τ_{res}. After steady shear at a high shear rate, the stress initially fell sharply to very small values, passed through a minimum, and then increased gradually approaching the residual stress value obtained in low-shear-rate tests. They also described the mechanism of this peculiar behaviour.

Very few dynamic oscillatory flow studies on ceramic compounds have been reported in the literature [26, 27]. Apparently, the dynamic behaviour of ceramic compounds is similar to that of highly particle-filled polymer systems. Payne [28–30] found that the dynamic moduli of carbon-black-filled rubber vulcanizates were strongly dependent on the strain amplitude; only at very low strains was the modulus independent of the strain. Gandhi and Salovey [31] reported that upon the addition of carbon black to a polymer melt, both G' and G'' become independent of the frequency and temperature at low frequencies, which corresponds to the yield behaviour in steady shear flow at low shear rates.

Rong and Chaffey [32] studied the effect of titanium-dioxide particles on the dynamic mechanical behaviour of polystyrene using a Weissenberg rheogoniometer. They found that the Cox–Merz rule [33] did not hold for the filled systems. However, several authors found that the steady-shear viscosity versus shear-rate curve coincides quite well with the large-amplitude envelope of the complex viscosity versus strain-rate-amplitude curve at various frequencies. This is known as the *modified Cox–Merz rule* [26]. This behaviour was first observed by Philippoff [34] on polymer solutions, Vinogradov *et al.* [35] on pure polymer systems and Isayev *et al.* [36, 37] on dispersed systems and bitumens.

Recently Doraiswamy *et al.* [26] proposed a non-linear model to describe the rheological behaviour of concentrated ceramic suspensions which exhibit a yield stress. Based on this analysis, a correlation has been proposed between the steady shear viscosity versus shear-rate curve and the complex viscosity versus strain-rate amplitude curve which is analogous to the Cox–Merz rule for viscoelastic materials. Oscillatory shear experiments for a 70 vol % suspension of silicon particles in polyethylene indicated good agreement between the data and the model predictions.

The purpose of this paper is to present an extensive rheological study of a ceramic-injection-moulding compound, namely a silicon powder with a polypropylene-binder system. This study covers steady, transient, and dynamic oscillatory shear flows. Particular attention is given to a low-shear-rate study where the yield behaviour, and some anomalous stress behaviour is observed in the measurements.

2. Experimental procedure

2.1 Materials

The material used in this study was silicon powder incorporated into a polypropylene binder. The silicon powder was of Silgrain grade (Elkem Metals) with a density of 2300 $kg\,m^{-3}$. The results of the measurements of the particle-size distribution are given in Table I, they indicate that the average particle size is 2.4 μm, with the largest particle being no greater than 10 μm. The loading was 82% by weight, or 65% by volume. The major binder was a polypropylene powder, 6462-HR (Microthene), with a melt index of 5.0 g per 10 min, and a density of 900 $kg\,m^{-3}$. The polypropylene loading was 12% by weight. The minor binder was stearic acid F-1000 (Harwick). The loading was 2.0% by weight. The processing aid was a dioctyl phthalate polycizer (DOP, Aldrich) with a density of 981 $kg\,m^{-3}$, and a loading of 4.0% by weight. According to the experimental studies by Edirisinghe and Evens [9] this ceramic compound was found to be one of the most promising injection-moulding compounds.

2.2 Sample preparation

The silicon powder was first pre-blended with stearic acid in a Henschel high-speed mixer at 3000 r.p.m (revolutions per minute), for 2 min in 1.5 kg batches. Then the major binder, polypropylene powder, and the minor binder, DOP, were added and mixed for another 2 min. Consequently, the mixture was compounded and pelletized using a co-rotating twin-screw

TABLE I Particle size distribution

Size (μm)	< 2	2–4	4–6	6–8	8–10
Percentage	45.0	30.6	11.6	11.8	1.0

extruder ZSK 30 (Werner & Pfleiderer) at 200 °C and 210 r.p.m.

To prepare the disk samples for the RMS-800, the compounded sample was compression moulded in a compression moulding press at 190 °C to form a flat sheet 2 mm thick. The sheet was then cut and polished into disks 25 mm in diameter.

2.3 Rheological measurements

2.3.1 RMS-800

Steady and transient shear tests in the low-shear-rate region, as well as the dynamic tests at various frequencies and amplitudes, were carried out on an RMS-800 with a parallel-plate fixture. The separation of the plates was 2 mm. It should be noted that use of cone-plate geometry for rheological measurements of ceramic-filled materials is inappropriate. During loading of the sample into the device a permanent breakage of the particle structure occurred especially in the area of the cone tip. Also, it was observed that substantial normal forces were generated during the sample loading. These forces did not relax until the imposition of a shearing flow. In addition, during rotation the ceramic material was expelled from the clearance between the cone and the plate, making rheological measurements impossible. All these undesirable effects were avoided in the parallel-plate fixture, but at the expense of non-uniformity of the shear-rate distribution in the radial direction.

To avoid thermal degradation of polypropylene at high temperatures, the tests were performed in a nitrogen environment. In order to prevent the evaporation of additives, such as stearic acid, a high-temperature grease was used to cover the edge of the sample disk. During the sample loading, a normal force was generated in the melt due to the compression force of the upper plate. After loading the sample, the normal force generated can hardly relax if no strong shear follows. The normal force held in the sample was found to have a strong influence on the test results. Therefore, it is important to maintain a certain normal-force value during the test in order to obtain good adhesion between the sample and the fixture, and to obtain good data reproducibility. In the present study, the initial normal force was kept at 600 g for 10 min. At this value of the normal force the dependence of the measured shear stress on the imposed normal force tends to level off. The testing temperature was 190 °C.

The measurements in steady mode included steady simple shear flow, transient start-up shear flow, and stress relaxation after cessation of steady shear flow. For steady shear flow and start-up shear flow, a constant shear rate was imposed on the sample by imposing a constant rotational speed on the lower plate. The torque was monitored until it reached an equilibrium value. Then the rotation was stopped and the change of the torque with time was recorded. Each data point on the flow curve was obtained using a fresh sample.

The measurements in dynamic mode included a frequency sweep, a strain sweep and stress relaxation after suddenly imposing a shear displacement. In the frequency-sweep test, the frequency changed within a pre-set range at a fixed temperature and strain amplitude. In the strain-sweep test, the dynamic-strain amplitude changed within a pre-set range at a fixed temperature and frequency. In both tests the torque and phase-angle change were measured. The storage modulus, G', the loss modulus, G'', the dynamic viscosity, η', the complex viscosity, η^*, and the loss angle, $\tan\delta$, were calculated. In step-shear experiments, the torque decay with time was monitored after a single, clockwise, step jump of the lower plate to a selected strain. The relaxation modulus, G, was calculated as a function of time.

2.3.2. Instron capillary rheometer

The steady-state measurements in the high-shear-rate range were carried out with an Instron capillary rheometer. A capillary of diameter $D = 1.5$ mm and length to-diameter ratio of $L/D = 28.7$ was used. The test temperature was 190 °C. A pre-heating time of 15 min was used to allow the material to reach thermal equilibrium. In order to avoid air bubbles being trapped in the sample, the material was fed into the barrel very slowly, and then it was firmly pressed. Since the load cell was mounted on the top of the plunger, the barrel-friction force must be taken into account. This effect becomes more evident when the material is highly filled. In order to eliminate the barrel effect, the plunger-force reading was taken, for each plunger speed, when the plunger was within a distance of 1–4 cm from the capillary die entrance. The large-amplitude force and flow-rate oscillations were observed in these experiments. The entrance corrections were neglected in the calculation of shear stress. The shear-rate calculations were based on the plunger speed without applying a Rabinowitch correction.

3. Results and discussion

3.1 Steady mode

The steady-shear-flow curves measured by the RMS-800 and the Instron capillary rheometer are shown in Fig. 1. An interesting phenomenon was observed while conducting the measurements with the RMS-800. At low shear rates (10^{-5}–10^{-3} s^{-1}), the shear stress decreased with increasing shear rate until it attained a minimum value. As the shear rate further increased, the stress value increased. A similar phenomenon was reported by Vinogradov and Malkin [16] on studies related to the rheology of greases.

A possible explanation for this anomalous phenomenon is as follows. The ceramic injection-moulding compound is highly filled with non-spherical, irregularly shaped particles. When the material is subjected to a very low shear rate (10^{-5} s^{-1}), the particle skeleton still holds. However, the very slow deformation rate may induce rearrangement of the particles to a higher order or to a more highly oriented structure. Therefore, at very low shear rates, the shear stress grew with time to a high value. This behaviour is called *work hardening* in the case of greases [16]. As the shear rate slightly increased (a fresh sample was used for each shear-rate test), the work hardening

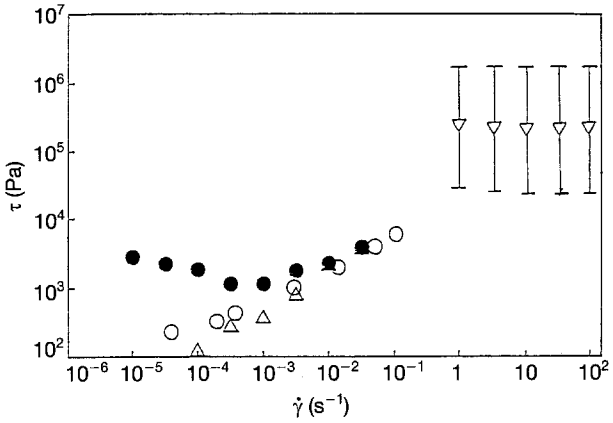

Figure 1 Shear stress as a function of shear rate for a silicon/polypropylene compound (65 vol %Si) at 190 °C using the following instruments: (○) co-axial cylinder, (●) RMS-800, (△) RMS-800 disturbed sample, and (▽) Instron capillary.

became less apparent, and the stress decreased to a minimum value. This minimum value is considered to be a yield value. As the shear rate further increased, the particle structure began to break down. The viscous drag became larger and larger due to the relative displacement of the layers of the binder and due to the fragments of the broken-down skeleton. Typical non-Newtonian behaviour can be seen in the high-shear-rate region.

The (△) data points in Fig. 1 were also obtained using the RMS-800, but with a disturbed sample. The sample was first subjected to an oscillation with a strain amplitude of 70% at a frequency of 1 s^{-1} for 5 min. Then the sample was tested under a steady shear. In this case, *work hardening* did not appear, and the stress value was much lower than that of the undisturbed sample at low shear rates. This reduction of the stress value depends on the extent of the disturbance which causes the destruction of the particle structure. At higher shear rates, the test result is consistent with the data obtained from the undisturbed sample. The test provides additional evidence for the mechanism of the anomalous phenomenon.

High-shear-rate tests were conducted in an Instron capillary rheometer. A typical stick–slip phenomenon was found at all the shear rates investigated ($\dot{\gamma}$ = 1–100 s^{-1}) as evidenced by the oscillations of the measured force. The steady-state-stress values and their oscillatory amplitudes are shown in Fig. 1. A plot of the plunger force oscillation with time is given in Fig. 2. When the plunger starts to go down, the plunger force begins to increase. At this stage, the extrudate comes out of the capillary at a very slow speed, and occasionally any motion of the extrudate can hardly be seen. As soon as the force of the plunger reaches the maximum value shown in Fig. 2, it drops dramatically to a minimum value. The drops in force were accompanied by an abrupt squirting of the extrudate. After squirting, the extrudate movement became so slow that it could hardly be seen. At the same time the force on the plunger increased again, and the next period began. When the extrusion speed was relatively low, severe melt fracture appeared at the tip of the extrudate upon squirting. At high speeds, the

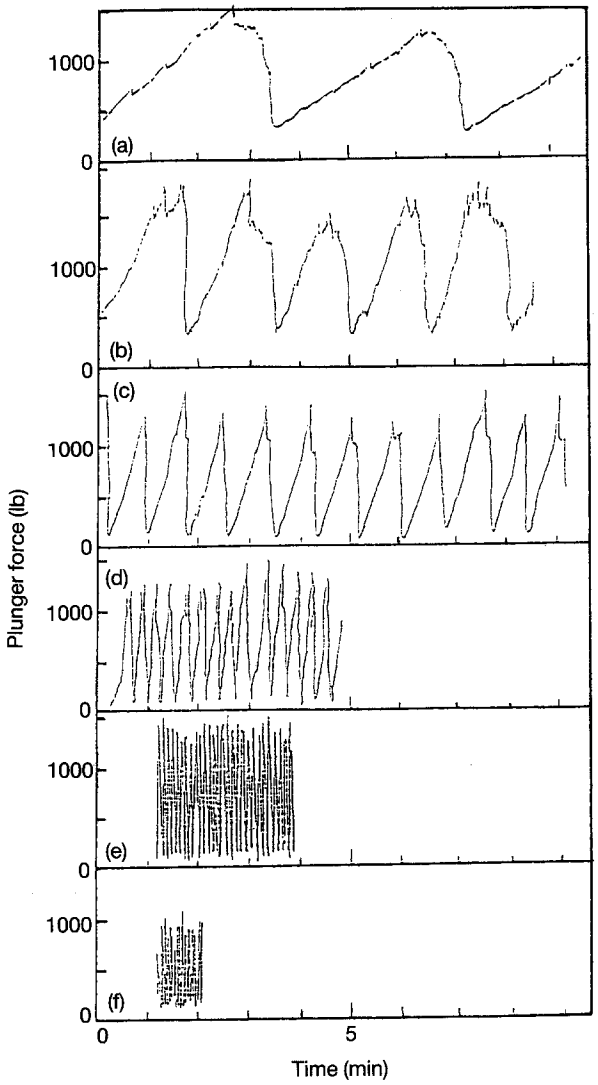

Figure 2 Plunger force oscillation during flow of a silicon/polypropylene compound in an Instron capillary rheometer for T = 190 °C and L/D = 10 for values of plunger speed of: (a) 0.03, (b) 0.1, (c) 0.3, (d) 1, (e) 3, and (f) 10 inch min^{-1}.

whole extrudate showed severe melt fracture. It was found that the amplitude of the force oscillation was almost constant for any plunger speed. However, the oscillating frequency proportionally increased with the plunger speed.

The results of transient shear stress are shown in Fig. 3 for start-up shear flow at various shear rates. As mentioned in the discussion of Fig. 1, because of the work-hardening phenomenon, the stress grew monotonically at small shear rates, $\dot{\gamma} = 10^{-5}$ and 10^{-4} s^{-1}, and the final equilibrium value was not attained. The stress overshoot began to appear when the shear rate was around 10^{-3} s^{-1}. As the shear rate further increased, the overshoot appeared at longer times.

The stress relaxations after cessation of steady shear flow are shown in Fig. 4. Another peculiar phenomenon was observed. At the lowest shear rate (10^{-5} s^{-1}), the stress relaxed slightly and slowly. As the shear rate increased to $\dot{\gamma} = 10^{-4}$ s^{-1}, the stress relaxed very little and after that it slightly increased. As the shear rate exceeded 10^{-3} s^{-1}, the stress value decreased quickly, going through a minimum value and then increasing. As the shear rate increased, the stress decreased more dramatically at the beginning,

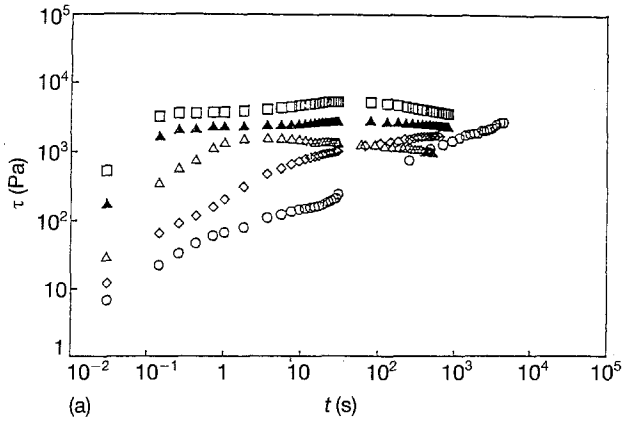

Figure 3 Transient start-up shear stress as a function of time for a silicon/polypropylene Si/PP compound (65 vol % Si) at 190 °C for $\dot{\gamma}$ values of: (○) $10^{-5}\,s^{-1}$, (◇) $10^{-4}\,s^{-1}$, (△) $10^{-3}\,s^{-1}$, (▲) $10^{-2}\,s^{-1}$, and (□) $3.163 \times 10^{-2}\,s^{-1}$.

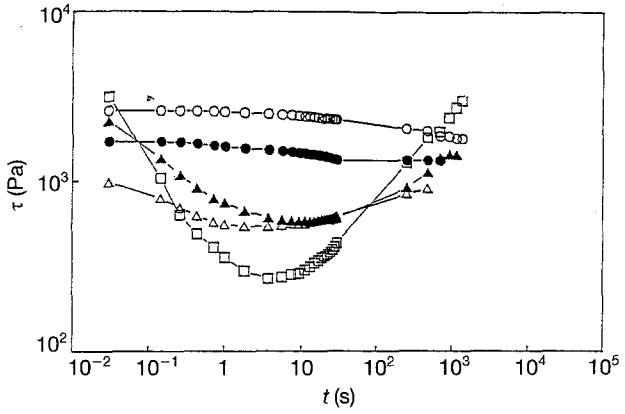

Figure 4 Shear stress as a function of time upon cessation of steady shear flow for a silicon/polypropylene compound (65 vol % Si) at 190 °C for $\dot{\gamma}$ values of (○) $10^{-5}\,s^{-1}$, (●) $10^{-4}\,s^{-1}$, (△) $10^{-3}\,s^{-1}$, (▲) $10^{-2}\,s^{-1}$, and (□) $3.163 \times 10^{-2}\,s^{-1}$.

then it rapidly increased and it eventually reached the value corresponding to the previous steady shear value.

The relaxation modulus after a sudden shear displacement is given as a function of time in Fig. 5. In a similar way to Fig. 4, when the initial displacement was very small ($\gamma_0 = 0.1\%$), the relaxation modulus decreased slowly in the initial stages and this was followed by a monotonic relaxation. As the displacement became larger ($\gamma_0 = 1.0\%$) the stress relaxed quickly in the initial stages, then it gradually tended to a constant value. As the displacement further increased, the stress dropped dramatically at the beginning, passed through a minimum value, and it finally increased. Qualitatively, the behaviour of the relaxation modulus shown in Fig. 5 is similar to that of the stress relaxation shown in Fig. 4 after cessation of steady shear flow.

Glushkov *et al.* [25] reported a similar relaxation phenomenon for highly filled polybutadiene. According to Glushkov *et al.*, this phenomenon is the result of elastic deformation of the elements of the ruptured structure during flow. The residual potential energy of these elements creates a new state of stress in the newly formed bonds after the flow ceases. However, the real

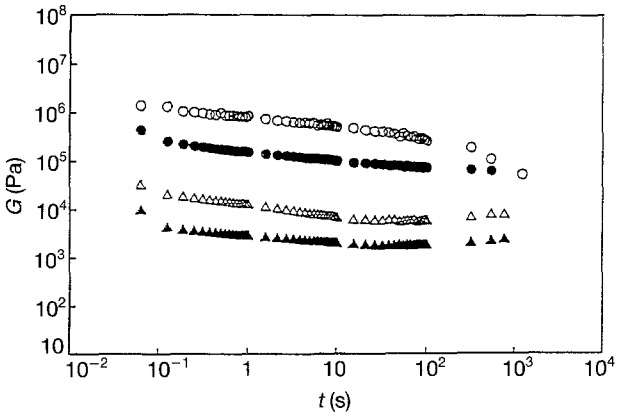

Figure 5 The relaxation modulus as a function of time after a sudden shear displacement for a silicon/polypropylene compound (65 vol % Si) at 190 °C for values of γ_0 of (○) 0.1%, (●)1.0%, (△) 10%, and (▲) 30%.

mechanism is still not clear, and more extensive experiments are needed in order to reasonably explain the observed phenomenon.

Fig. 6a gives the results of transient start-up shear viscosity and Fig. 6b gives the consequent stress relaxation after cessation of steady shear flow at a fixed shear rate. This start-up and relaxation test was repeated three times on the same sample. The observation time for start-up shear flow tests was 35 min, and for stress relaxation tests it was 25 min. The rest time

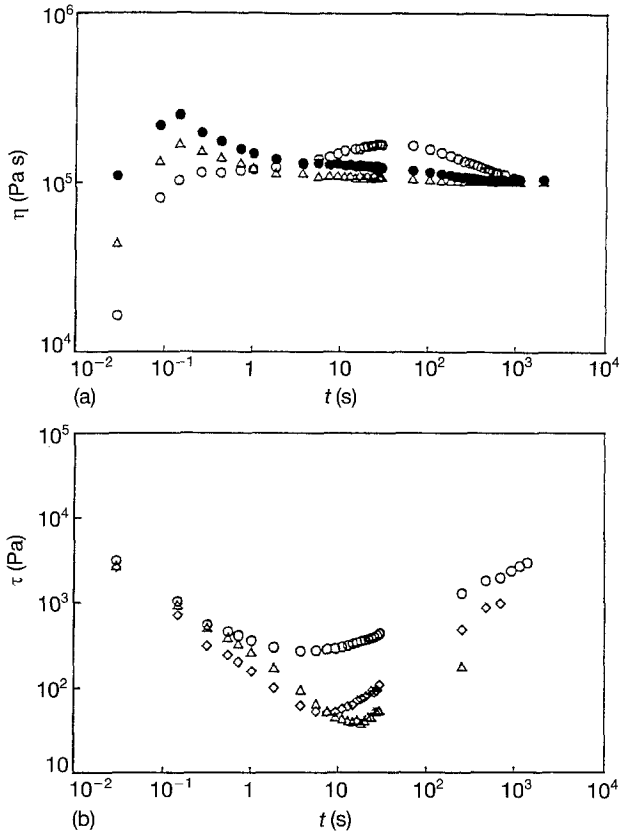

Figure 6 (a) Transient start-up shear viscosity (65% vol% Si) at 190 °C (○) first run, (●) second run, and (△) third run; and (b) stress relaxation upon cessation of steady shear flow (○) first run, (◇) second run, and (△) third run. Both are given as a function of time for a silicon/polypropylene compound with $\dot{\gamma} = 3.163 \times 10^{-2}\,s^{-1}$.

between various runs was 25 min. The stress overshoot in the first run appeared at a longer time compared to those in the second and third runs. The overshoot value of the first run was even less than that of the second run. This peculiar behaviour suggests the possible existence of a transient structure (rearrangement of particles) in the material during deformation. In the first run it took a long time to disturb or break the structure. In the second and third runs the transient structure had been broken down. It appears that this transient structure exhibits higher strength than the initial structure, this is evidenced by the higher value of the stress overshoot in the second run. However, this transient structure is more brittle than the initial structure, so that the viscosity overshoots in the second run appear earlier in time than in the first run. In the third run the value of the overshoot decreased compared to the second run.

Fig. 6b shows the stress-relaxation curves after cessation of the steady shear flows during these three runs. The three relaxation curves are similar in shape but show different values despite the fact that the relaxation process started from the same steady-state value of the shear stress. In all the runs, the stress relaxed to a minimum value and then it increased. The minimum value decreased for each subsequent run, and its position on the time scale shifted towards longer times. The rate of stress decay before the minimum and the rate of stress growth after the minimum increased with each subsequent run. It can be expected that if the test is repeated a few more times, the relaxation curve will finally return to normal, that is, it will monotonically decrease for a longer time. This indicates that the transient structure is gradually destroyed in each subsequent run and that its recovery takes a longer time.

3.2. Dynamic mode

Typical dependencies of shear stresses on time during the oscillatory flow are shown in Fig. 7 at a strain amplitude of 0.1 and at two frequencies, 0.0316 and $10\,s^{-1}$. It can be seen that the stress responses are slightly distorted from sinusoidal stresses. This is due to the non-linear behaviour of ceramic compounds. Such behaviour is observed over a range of amplitudes and frequencies. Thus, the values of G', G'' and η^* presented below are based on the first harmonics of stresses.

The results of the measurements of G', G'' and η^* in the dynamic-strain sweep test at various frequencies are given in Fig. 8a, b and c, respectively. Non-linear behaviour can be observed in the whole strain range tested. As the strain increased, the values of G' and G'' slightly decreased. The decrease of G' and G'' with the strain amplitude became somewhat less pronounced when the frequency increased. This indicates that the particle structure of this compound is more easily destroyed at low frequencies than at high frequencies. This observation is evidently related to the characteristic time of structure breakdown and recovery; it can be explained as follows. In the oscillatory shear flow, structure breakdown and recovery takes place during

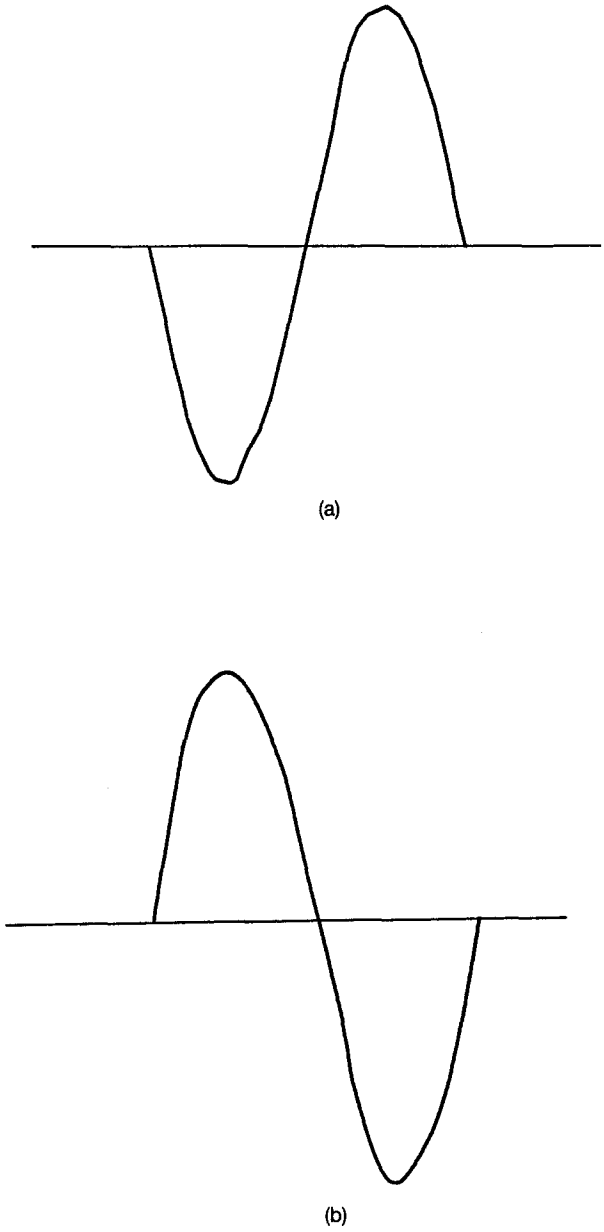

Figure 7 Typical dependencies of shear stresses on time during oscillatory shear flow of a silicon/polypropylene compound: (a) $\omega = 0.0316\,s^{-1}$ and $\gamma_0 = 0.1$, and (b) $\omega = 10\,s^{-1}$ and $\gamma_0 = 0.1$.

every cycle. At low frequencies, the cycle time is sufficiently large to allow for structure recovery during each cycle. At high frequencies, the cycle time is too short and the structure cannot recover, so that it attains its equilibrium state. Thus, the structural changes become less sensitive to frequency, as is observed in the experiments at high frequencies.

Fig. 9 shows the frequency dependencies of G', G'' and η^* at a small strain ($\gamma_0 = 0.3\%$). It is evident that G' and G'' increased very slowly with frequency, so that the whole curve can be considered to be close to the plateau region corresponding to yielding. In addition, the η^*–ω curve is a straight line with a slope close to -1 on the log–log scale which also suggests that the material is in a state close to yielding. A comparison of a curve of η^* versus ω (Fig. 9) and η versus $\dot{\gamma}$ (obtained from Fig. 1) suggests that $\eta^* \gg \eta$ at $\omega = \dot{\gamma}$, indicating that an empirical Cox–Merz rule is not valid for the material under consideration.

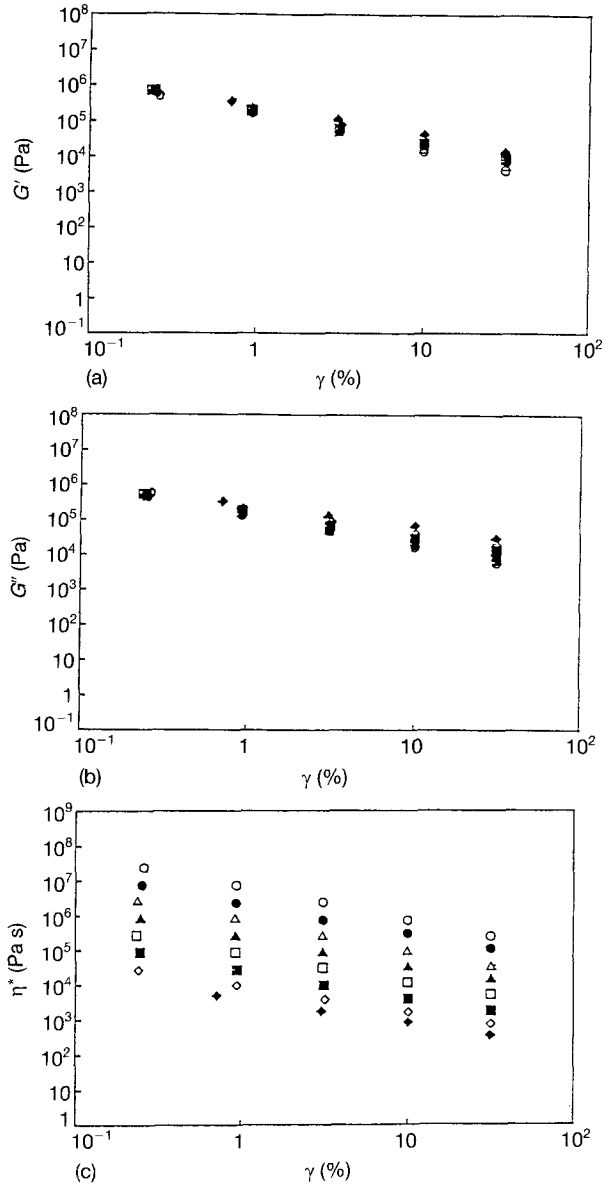

Figure 8 (a) Storage modulus, (b) loss modulus and (c) complex viscosity as a function of the strain amplitude at various frequencies for a silicon/polypropylene compound (65 vol % Si) at 190 °C for the following values of ω: (○) 0.0316 s^{-1}, (●) 0.10, (△) 0.316, (▲) 1.00, (□) 3.16, (■) 10.0, (◇)31.6, and (◆) 100.0.

A comparison of the steady shear viscosity versus shear rate (η–$\dot{\gamma}$) curve and the complex viscosity versus strain-rate amplitude (η^*–$\gamma_0\omega$) curve at various frequencies is given in Fig. 10. As the dynamic data show, the right-hand portion of each curve (that is, the non-linear region of the curve corresponding to each frequency at large amplitudes) tends to form a unique envelope. This envelope coincides well with the curve of steady shear viscosity, η–$\dot{\gamma}$, measured by the RMS-800, indicating that $\eta = \eta^*$ at $\dot{\gamma} = \gamma_0\omega$. The latter is the basis for the *modified Cox–Merz rule* first observed by Phillippoff [34] and later by others (see Section 1). In particular, for ceramic compounds, this correlation is observed at values of strain as low as 5% which is much lower than in polymer solutions and melts [27]. The latter is possibly due to the fact that ceramic compounds are brittle and are not viscoelastic materials in the usual sense, while polymeric solutions and melts are viscoelastic and exhibit high elastic strains.

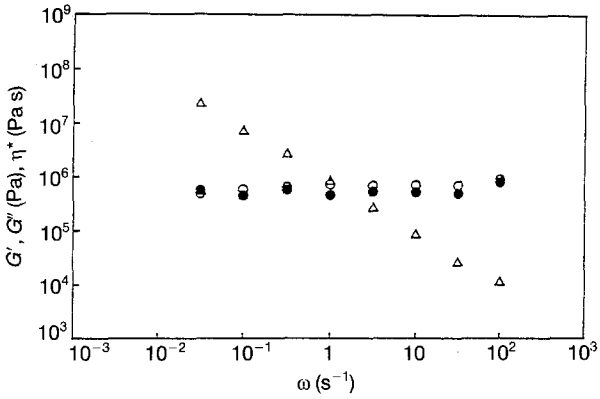

Figure 9 (○) Storage modulus, (●) loss modulus and (△) complex viscosity as functions of frequency at low strain amplitude for a silicon/polypropylene compound (65 vol % Si) at 190 °C.

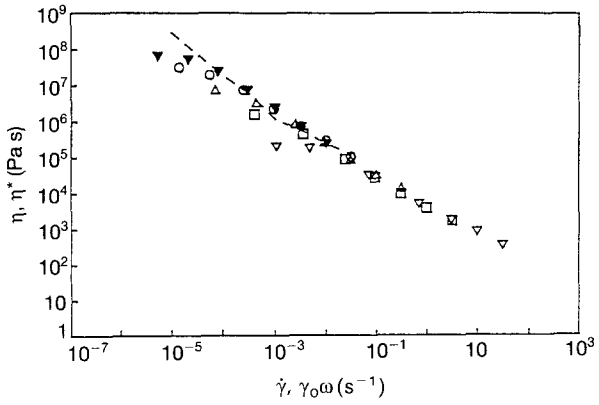

Figure 10 (– – –) The steady shear viscosity as a function of the shear rate and the complex viscosity as a function of the strain-rate amplitude at various frequencies for a silicon/polypropylene compound (65 vol % Si) at 190 °C: (○) 0.10 s^{-1}, (△) 1.00 s^{-1}, (□) 10.0 s^{-1}, (▽) 100.0 s^{-1}, and (▼) 0.0316 s^{-1}.

This finding is of special importance since difficulties arise in the steady-shear-viscosity measurements in the intermediate-shear-rate region due to melt fracture and flow instability. Measuring difficulties, such as wall slip, stress oscillation, and stick–slip behaviour are also encountered in the high-shear-rate region using a capillary rheometer. In these cases, dynamic measurements and the *modified Cox–Merz rule* may provide the steady-shear-viscosity information.

4. Conclusions

1. When the ceramic compound was tested using the RMS-800 instrument with parallel plates, work-hardening phenomenon was observed in the low-shear-rate region ($\dot{\gamma} < 10^{-4}$ s^{-1}). Due to this effect, a minimum stress value appeared in the steady-shear-flow curve, which indicated the existence of a yield stress value.

2. During the Instron-capillary-rheometer tests in the shear-rate region from $\dot{\gamma} = 1$–100 s^{-1}, the shear stress was found to oscillate and melt fracture occurred. The mean stress value and the oscillating amplitude at any plunger speed were almost constant. The frequency of oscillation increased as the extrusion

speed increased. Evidently, a critical stress value existed which could not be exceeded. This led to shear-stress oscillations.

3. In the repeated start-up-shear-flow measurements, the stress overshoot in the first run appeared at a longer time than in successive runs. The value of the overshoot in the second run was larger than that in the first run and it appeared at an earlier time.

4. In stress relaxation upon cessation of steady shear flow in the intermediate-shear-rate range ($\dot{\gamma} = 10^{-3}$–$3.16 \times 10^{-2}\ s^{-1}$), the stress first relaxed, it passed through a minimum value and then it increased.

5. In strain-sweep tests, all the dynamic properties, G', G'', η^* and $\tan\delta$, displayed highly non-linear behaviour, even at the smallest strain amplitude tested. This non-linearity is due to the structural change which occurs when the material is subjected to a strain. This structural change is more sensitive to low frequencies.

6. In frequency sweep tests at small strains, G', G'' and $\tan\delta$ exhibited a plateau. The slope of η^* versus ω is close to -1 in the low-frequency region. All these observations imply the existence of a yield value.

7. The usual empirical Cox–Merz rule is not valid for this material. In the highly non-linear region, the envelope of the η^*–$\gamma_0\omega$ curve at various frequencies coincides well with the steady shear, η–$\dot{\gamma}$, curve at $\dot{\gamma} = \gamma_0\omega$.

8. All the above anomalous phenomena are related to the possibility of the existence of a special particle structure due to the very high particle loading and the particle characteristics.

References

1. J. A. MANGELS and W. TRELA, *Adv. Ceram.* **9** (1984) 220.
2. B. C. MUTSUDDY, *J. Ind. Res. Dev.* **25** (1983) 76.
3. F. MOORE, "Rheology of ceramic systems", (Maclaren, London, 1965), Ser. 2.
4. A. I. ISAYEV, *Adv. Ceram.* **21** (1987) 601.
5. M. A. STRIVENS, *Amer. Ceram. Soc. Bull.* **42** (1963) 13.
6. A. C. ANDERS, jr, *Ceram. Engng. Sci. Proc.*, **8** (1987) 11.
7. E. C. BINGHAM, "Fluidity and Plasticity" (McGraw Hill, New York, 1922).
8. B. C. MUTSUDDY, *Ind. Ceram.* **839** (1989) 436.
9. M. J. EDIRISINGHE and J. R. G. EVENS, *J. Mater. Sci.* **22** (1987) 269.
10. A. M. LITMAN, N. R. SCHOTT and S. W. OZLOWSKI, *SPE Tech. Papers* **22** (1976) 549.
11. K. UMEYA, *J. Soc. Rheol. (Japan)* **13** (1985) 145.
12. R. W. MYERHOLTZ, *J. Appl. Polym. Sci.* **11** (1967) 687.
13. J. M. LUPTON and J. W. REGESTER, *SPE J.* October (1965) 235.
14. U. YILMAZER and D. M. KALYON, *J. Rheol.* **33** (1989) 1197.
15. A. I. LEONOV, *Rheol. Acta* **23** (1984) 591.
16. G. V. VINOGRADOV and A. Y. MALKIN, "Rheology of polymers" (Mir, Moscow, 1980).
17. J. L. WHITE, "Polymer compatibility and incompatibility principles and practices", Vol. 2 (Harwood Academic, New York, 1982).
18. J. T. BERGEN, in "Processing of thermoplastic materials", edited by E. C. Bernhardt (Reinhold, New York, 1959).
19. J. M. McKELVEY, "Polymer processing", (Wiley, New York, 1962).
20. Z. TADMOR and C. G. GOGOS, "Principles of polymer processing", (Wiley, New York, 1962).
21. S. C. TSAI and K. ZAMMOURI, *J. Rheol.* **32** (1988) 737.
22. V. M. LOBE and J. L. WHITE, *Polym. Engng. Sci.* **19** (1979) 617.
23. S. MONTES, J. L. WHITE and N. NAKAJIMA, *J. Non-Newt. Fluid Mech.* **28** (1988) 183.
24. D. CHAN and R. L. POWELL, *J. Non-Newt. Fluid Mech.* **15** (1984) 165.
25. I. A. GLUSHKOV, G. V. VINOGRADOV and V. A. ROZHKOV, *Mekhanika Polimerov, (USSR)* **5** (1974) 902.
26. D. DORAISWAMY, I.-L. TSAO, S. C. DANFORTH, A. N. BERIS and A. B. METZNER, Proceedings of the Tenth International Congress of Rheology Vol. 1 (1988) pp. 300–302.
27. D. DORAISWAMY, A. N. MUJUMDAR, I. TSAO, A. N. BERIS, S. C. DANFORTH and A. B. METZNER, *J. Rheol.* **35** (1991) 647.
28. A. R. PAYNE, *J. Appl. Polym. Sci.*, **3** (1960) 127.
29. *Idem. ibid.* **6** (1962) 57.
30. *idem., ibid.* **6** (1963) 873.
31. K. GANDHI and R. SALOVEY, *Polym. Engng Sci.* **28** (1988) 1628.
32. S. RONG and C. E. CHAFFEY, *Rheol. Acta* **27** (1988) 179.
33. W. P. COX and E. H. MERZ, *J. Polym. Sci.* **28** (1958) 619.
34. W. PHILIPPOFF, *Trans. Soc. Rheol.* **10** (1966) 317.
35. G. V. VINOGRADOV, YU. G. YANOVSKY and A. I. ISAYEV, *J. Polym. Sci. A8* (1970) 1239.
36. A. I. ISAYEV, G. YU, V. G. YANOVSKY, VINOGRADOV and L. A. GORDIEVSKY, *J. Engng Phys.* **18** (1970) 675.
37. A. I. ISAYEV, V. A. ZOLOTAREV and G. V. VINOGRADOV, *Rheol. Acta* **14** (1975) 135.

Received 6 April
and accepted 6 October 1993